

# UTILIZATION OF TANDEM-X DEM FOR TOPOGRAPHIC CORRECTION OF SENTINEL-2 SATELLITE IMAGE

Sharad Kumar Gupta, PhD Scholar  
Dericks P. Shukla, Assistant Professor  
School of Engineering,  
Indian Institute of Technology, Mandi,  
Himachal Pradesh, India  
[sharadgupta27@gmail.com](mailto:sharadgupta27@gmail.com)  
[dericks@iitmandi.ac.in](mailto:dericks@iitmandi.ac.in)

## ABSTRACT

Topographic shadows of irregular mountains obstruct the analysis of satellite images in hilly areas. Topographic shading creates ambiguity among different elements of scene having similar hue and saturation but different intensities, which leads to misinterpretation of surface features. Due to this effect, there is high variability in the reflectance response of similar vegetation types i.e. sunny areas show more than actual reflectance, whereas shaded areas show less than expected reflectance. In this paper, the effects of digital elevation model (DEM) has been assessed on topographic correction of Sentinel-2 satellite images. TanDEM-X digital elevation model with spatial resolution of 12 meters is used in the study. DEMs was resampled at 10 meters to match the spatial resolution of satellite image. In this research work, six known methods of corrections are compared: the cosine, semi-empirical C, Minnaert, C-Huang Wei, SCS + C and VECA correction depending on the solar incidence angle and exitance angle. Correlations and linear regressions between reflectance values of satellite image and topographic parameters (slope, aspect derived from DEM) are investigated. Ideally, the slope of regression line between illumination condition and image band should be zero, as topography should not control the solar illumination over terrain. However, in hilly regions, topography plays a critical role by controlling the amount of sunlight falling on north and south faces of mountains. Hence, after application of topographic correction methods, this slope of regression line decreases. Coefficient of variation, mean and standard deviation was used for the statistical analysis of the results obtained after topographic correction. The results of the study shows that classical cosine method overcorrect the image. As seen from the statistical analysis, VECA correction method provides good correction of topography. However, the C-Huang Wei, Minnaert, C and SCS + C-correction methods yielded an impressive reduction in the visual topographic effects.

**KEYWORDS:** topographic correction, TanDEM-X, radiometric correction, illumination correction, digital elevation model.

## 1. INTRODUCTION

The topography of an area is an important factor. It plays a critical role in determining the land surface reflectance, which in turn affects the quantitative analysis of remotely sensed data. In topographically undulated areas, variation in illumination angles and reflection geometry are caused by different slope angles and orientations (Colby 1991). Due to this effect, there is high variation in the reflectance pattern or reflectance curve for similar types of vegetation i.e. sunny areas appears brighter than shaded areas for similar vegetation (Riaño et al. 2003). This situation is shown in Figure 1.

Terrain orientation varies throughout the topography in an area. It creates variation in the signal received from similar land cover features because of differences in solar irradiance and radiance, according to the angle of incident, angle of illumination and exitance respectively (Soenen et al. 2005). Topography cannot control the sun-crown geometry, as the trees are perpendicular to the geoid. This leads to shadow effect in the mountainous regions. As the satellite sensor measures the collective radiance of all trees inside their IFOV, the canopy

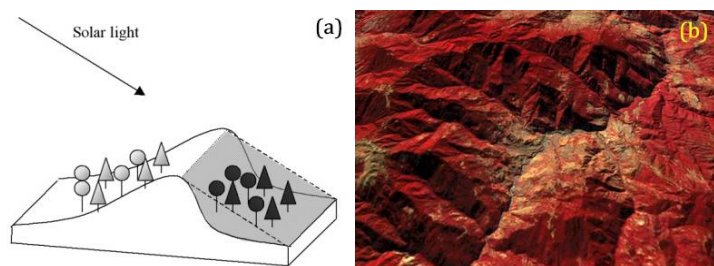


**Figure 1.** (a) Effect of Topography on reflectance (b) Effect of topography on Kedar Valley, Uttarakhand, India (Landsat 7 False colour composite image draped over ASTER 30m DEM, Source: USGS).

shadowing (and hence the topography) strongly controls the canopy brightness at the pixel scale (Gu et al. 1998). The topographic correction methods can be divided into two types viz. physics based methods and data based empirical methods (Li et al. 2017). The physics based model depend on radiative transfer models and considers the effects of topography as well as atmospheric conditions at the time of acquisition of data (Balthazar et al. 2012). These are very accurate but highly complicated methods. Hence, they are not widely used as getting those parametric data at the time of acquisition is very difficult. So empirical methods are more popular as it uses topographic data such as digital elevation model (DEM) and statistical information from the satellite images for correction of topographic effects (Civco 1989; Teillet et al. 1982). However the spatial resolution of DEM plays a critical role in these data based topographic correction models. It is advised to use a DEM that have similar spatial resolution, as that of the satellite image that needs to be corrected (Richter et al. 2009; Meyer et al. 1993; Riano et al. 2003; Nichol et al. 2009; Gao et al. 2009a). However Hantson et al. 2011 have advised that DEM with pixel size equal to 1/3<sup>rd</sup> of the pixel size of the satellite image is required for better correction of topographic effects. There are various topographic correction models, such as Band ratio (Colby 1991), backward radiance correction transformation (Colby 1991), Minnaert method (Smith et al. 1980; Colby 1991; Pimple et al. 2017), Cosine correction (Teillet et al. 1982; Riano et al. 2003), C correction (Teillet et al. 1982; Hantson et al. 2011), sun–canopy–sensor (SCS) correction (Gu et al. 1998; Soenen et al. 2005; Fan et al. 2014), that have been used widely for correction of topographic effects in Landsat series satellites as well as Ikonos images. An empirical method called Variable Empirical Correction Algorithm (VECA) for correction of topographic effects from Landsat 7 ETM+ image has also been widely used (Gao et al. 2007; Gao et al. 2009b). A stratified approach for topographic correction of medium resolution satellite image has also been developed (Szantoi et al. 2013).

All multi-temporal change detection algorithms depend on comparing an image from different dates assuming that those images are geometrically corrected & radiometrically consistent. For radiometric correction of multi-temporal images, topographic correction is especially critical for any study area with rugged terrain, since illumination conditions change along with seasonal sun zenith angle (Hantson et al. 2011). Hence, before performing any analysis on these satellite images, they must be corrected for topographic effects.

## 2. MATERIALS AND METHODS

### 2.1 Study Area & Data Resources

Mandi sub-district of Himachal Pradesh, India, is chosen as the study area having the central point coordinates of 31°41' N Latitude and 76°57' E Longitude as shown in Figure 2. Mandi is nestled in the Shivalik Range of the Himalayas and has highly rugged topography which provides an optimal location for topographic correction studies. Sentinel-2 satellite image at spatial resolution 10 m was acquired on April 10, 2017 for carrying out the topographic correction studies in this area. The image was freely downloaded from the European Space Agency's Copernicus open access hub (<https://scihub.copernicus.eu/dhus/>). TanDEM-X elevation model with spatial resolution of 12 m was provided by DLR Germany via TanDEM-X Science Service System (<https://tandemx-science.dlr.de>). The details of the image and DEM used for the region are given in Table 1.

**Table 1. Data products used in this work**

S. No.	Type	Resolution	Satellite / Mission	Area	Date of Acquisition
1.	Satellite Image	10 meter	Sentinel 2	Mandi	10/04/2017
2.	DEM	12 meter	TerraSAR/ TanDEM	Mandi	-----

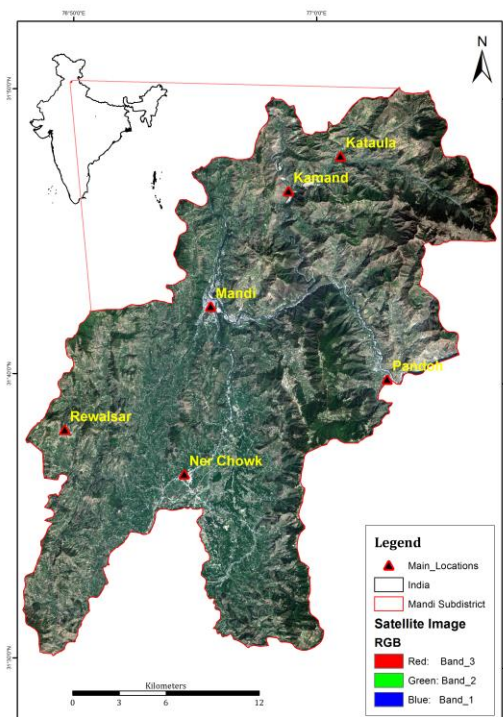


**Figure 2.** Natural colour composite image of Sentinel-2 satellite for the study area of Mandi sub-district, HP, India. [Source: Satellite Image (Earth Explorer, USGS), Boundary of India (Survey of India)]

## 2.2 Image Preprocessing

Digital numbers (DN) of satellite images are converted to reflectance values for establishing the relationship between illumination condition value and reflectance of an image for topographic correction analysis. Hence, scaled integer values, which range from 0 to 65,535 for Sentinel-2 (radiometric resolution 16 bit), are converted to the reflectance values using the quantification value given in metadata.

$$\rho_\lambda = \frac{DN}{Q}$$

Where  $\rho_\lambda$  = TOA Spectral Reflectance (Unit less), DN = Scaled integer values of pixels in image, Q = Quantification Value (from the metadata).

## 2.3 Topographic Correction

Topographic normalization is performed by modelling illumination condition (IL) with the DEM of same spatial resolution as that of the image to be corrected (Jenson 2005). The Tan-DEM is used for calculating incident angle ( $\gamma_i$ ) which is defined as the angle between the normal to ground and solar beam. IL values varies from -1 to +1 (Riaño et al. 2003) where  $IL < 0$  shows shadowed slopes which do not receive irradiance (Ekstrand 1996). Angles involved in the calculation of IL are shown in Figure 3. Illumination condition can be calculated using the mathematical equation given below.

$$IL = \cos \gamma_i = \cos \theta_p \cdot \cos \theta_z + \sin \theta_p \cdot \sin \theta_z \cdot \cos(\varphi_a - \varphi_o)$$

Where  $\gamma_i$  = local solar incident angle,  $\theta_p$  = slope angle,  $\theta_z$  = solar zenith angle,  $\varphi_a$  = solar azimuth angle,  $\varphi_o$  = aspect angle, solar zenith angle  $\theta_z = 90^\circ - \text{Solar elevation}$ . From the computed illumination condition (IL), different topographic correction methods, given in Table 2, are used to estimate flat normalized reflectance for each pixel.

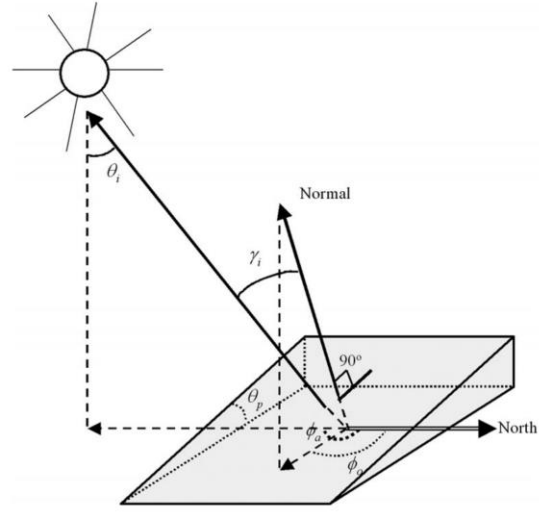


**Figure 3.** Angle involved in calculation of illumination condition (IL) required for topographic correction (Source: Riaño et al., 2003).

**Table 2. Details of topographical correction methods used in the study**

S. No.	Method	Characteristics	Mathematical Formula	References
1.	Cosine Correction	Wavelength-independent model	$\rho_H = \rho_T \left( \frac{\cos \theta_z}{IL} \right)$	Teillet et al., 1982
2.	C-Huang Wei Correction	Wavelength-independent model	$\rho_H = (\rho_T - \rho_{T_{min}}) \cdot \left( \frac{\cos \theta_z - IL_{min}}{IL - IL_{min}} \right) + \rho_{T_{min}}$	HuangWei et al., 2005
3.	VECA Correction	Wavelength-dependent model	$\rho_H = \rho_T \left( \frac{\bar{\rho}_T}{m * IL + b} \right)$	Gao et al., 2009
4.	Minnaert Correction	Wavelength-dependent model (wavelength independent models for Lambertian model)	$\rho_H = \rho_T \left( \frac{\cos \theta_p}{IL^{K_k} * \cos \theta_p^{K_k}} \right)$	Smith et al., 1980
5.	C-Correction	Wavelength-dependent model	$\rho_H = \rho_T \left( \frac{\cos \theta_z + C_k}{IL + C_k} \right)$	Teillet et al., 1982
6.	SCS + C Correction	Wavelength-dependent model	$\rho_H = \rho_T \left( \frac{\cos \theta_z * \cos \theta_p + C_k}{IL + C_k} \right)$	Soenen et al., 2005

Where,  $\rho_H$  = reflectance of horizontal surface,  $\rho_T$  = reflectance of inclined surface,  $K_k$  = Minnaert constant for band k (If  $K=1$ , Lambertian Surface), m and b = slope and intercept of regression line between IL and  $\rho_T$  and  $C_k = b/m$ .

The cosine correction (Teillet et al. 1982) neglects the diffuse irradiance and considers the solar zenith angle and the local solar incident angle for computation of the local illumination. The reflectance of the surface is calculated using the formula given in Table-1. Like Cosine method, C-HuangWei method also follows Lambertian assumption and is wavelength independent. VECA method was proposed by (Gao et al. 2009b) and is based on the theoretical and statistical analysis of the reflectance of the image. Minnaert (1941), who initially proposed a semi-empirical equation for describing the roughness of the moon's surface, called as a Minnaert correction. However, Minnaert method which uses the slope angle is called as Minnaert method with slope, was proposed by Smith et al. 1980. Minnaert coefficient  $K_k$  for each band can be obtained from the regression from below equation.

$$\ln(\rho_T * \cos\theta_p) = \ln(\rho_H) + K_k \ln(\cos\theta_p * IL)$$

Where  $K_k$  = Minnaert constant for band k. The term K models the non-Lambertian behavior. If  $K = 1$ , surface behaves as perfect Lambertian surface.

C-correction proposed by Teillet et al. 1982 is the modified form of Cosine correction which uses an empirical parameter 'C', for the correction of indirect irradiance to the incident solar flux over undulating terrain. The SCS correction is equivalent to projecting the sunlit canopy from the sloped surface to the horizontal, in the direction of illumination (Soenen et al. 2005). In the C and the SCS+C correction models, the C can be calculated based on the linear relationship between the original reflectance and the cosine of the solar incident angle.

$$\rho_T = m * IL + b$$

$$C_k = b/m$$

## 2.4 Methodology

Topographic correction requires elevation for illumination correction over the shadow regions of the satellite images. Hence, DEM was resampled at the 10 m to match the spatial resolution of the Sentinel-2 image (Bands 2, 3, 4 and 8). Afterward, slope (in degrees) and aspect are calculated from DEM using Horn's method. Parameters required for topographic correction such as solar zenith angle, azimuth angle are taken from image metadata provided. Image DN values are converted into reflectance using the method discussed in *Image Pre-processing step*.

For finding the band specific correction coefficients for VECA, Minnaert, C and SCS + C methods, linear regression analysis is performed between IL and near infrared band of satellite image. The slope of regression line shows the effect of topography on the image. All the methods for topographic correction are implemented in MATLAB. After correction of the image, regression analysis is again performed between corrected reflectance value and IL to check the slope of the corrected image; Statistical parameters such as mean, standard deviation and coefficient of variation are also calculated to compare all the methods.

## 2.5 Assessment of Topographic Correction Methods

The performance of the methods was assessed by comparing original Sentinel 2 (Band 2, 3, 4 and 8) image and the corrected image, using statistical assessment and visual interpretation (Pimple et al. 2017).

**2.5.1 Statistical Assessment.** The performance of the topographic correction methods is assessed using mean and standard deviation ( $\sigma$ ) of individual Sentinel-2 bands. A good correction method should decrease the inter-band variability, whereas mean value of each band should be very close to each other (Pimple et al. 2017). There should be reduction in the relative variability in comparison to the uncorrected image bands. The reduction in topographic shadow effects is shown by change in  $\sigma$  values. Reduction of  $\sigma$  of the reflectance was calculated by the coefficient of variation (CV). CV is the ratio of the  $\sigma$  to the  $\mu$ , expressed as a percentage (Pimple et al. 2017)

$$CV (\%) = \frac{\sigma}{\mu} * 100$$

Where CV = coefficient of variation,  $\sigma$  = standard deviation of reflectance values, and  $\mu$  = mean of the reflectance values. After the topographic correction, the CV should decrease.

**2.5.2 Visual Interpretation.** Visual interpretation was used for the assessment of the quality of corrected and original image. The effect of correction can be seen from the visual indication of corrected images. Mostly, noticeable or small differences could be observed in the true colour, false colour composites.

### 3. RESULTS & DISCUSSIONS

DEM was resampled at the 10 m to match the spatial resolution of the Sentinel-2 image (Bands 2, 3, 4 and 8). The resampled DEM was used for computing the slope gradient and aspect. Slope and aspect are calculated from DEM using Horn's method. Afterwards, Illumination condition variable IL was calculated. Data required for topographic correction are shown in Figure 4.

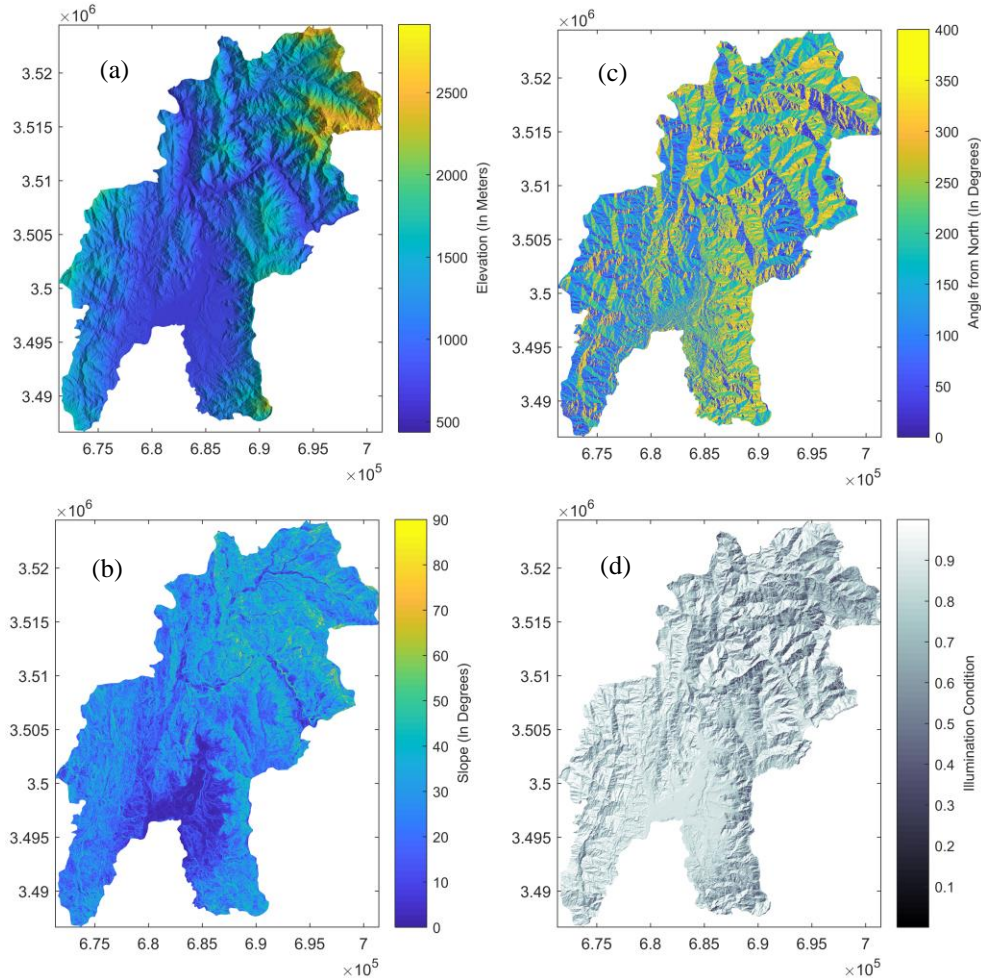


**Figure 4.** (a) Digital elevation model; (b) Slope (degree); (c) Aspect; (d) Illumination correction.

A strong correlation exists between the reflectance of pixels in the satellite data and the topographic variable IL over rugged terrain. Ideally, for flat terrain the linear regression between image reflectance values and topographic variable  $\cos i$  or IL has no slope, if any, due to variability of topography. After applying topographic correction methods, spectral differences between original and topographic normalized image should be low, otherwise, it would be a sign of over or under correction.

When topographic effects have been corrected, the correlation coefficient of reflectance and IL for each band will decrease and similarly, the slope of the fitted line will decrease. From curve fitting parameters, it is observed that slope of the line between IL & reflectance for VECA correction is least amongst all methods tested for topographic correction. C and C-HuangWei correction has slope nearly equal to VECA correction. The relation between IL and reflectance for the corrected and original image is shown in Figure 5, and regression parameters are given in Table 3. The curve fitting results obtained from the cosine method and Minnaert method are negative whereas positive for all the other methods. This method does not require any external parameters. It strongly overcorrects the influence of direct irradiance in areas of high incident angles and is therefore problematic for steep and sun-averted slopes, which appear brighter than sun-facing slopes. Cosine correction did not perform well & overcorrected the image (provided false illumination to areas of

low illumination). This is possibly due to overcorrection applied on the pixels with smaller IL values.

Lesser amount of slope of the line indicates better correction. Hence it can be seen from table 3 that VECA and C correction has lowest slope of 0.002 and 0.0030 respectively. This indicates that both these methods perform better and yield nearly similar results, which is also visible in the Figure 6. C-Huang Wei, and SCS + C also had nearly flat slope indicating good correction, however they did not perform as well as C and VECA method for topographic correction of Mandi region. Areas of low illumination are corrected largely. As these are non-Lambertian methods, which assume that the combination of the angles of incidence and observation can affect reflectance, and that surface roughness is also an important factor. These methods did not provide any false illumination over any area.

**Table 3. Slope and intercept for relation b/w illumination condition and Reflectance (NIR Band) for all correction methods**

S. No.	Methods	Parameters	
		Slope (m)	Intercept (b)
1.	Original Image	0.1797	0.1022
2.	Cosine Correction	-0.3622	0.5683
3.	C-Huang Wei Correction	0.0065	0.2541
4.	VECA Correction	0.0028	0.2376
5.	Minnaert Correction	-0.0254	0.2940
6.	C Correction	0.0030	0.2571
7.	SCS + C Correction	0.0428	0.2081

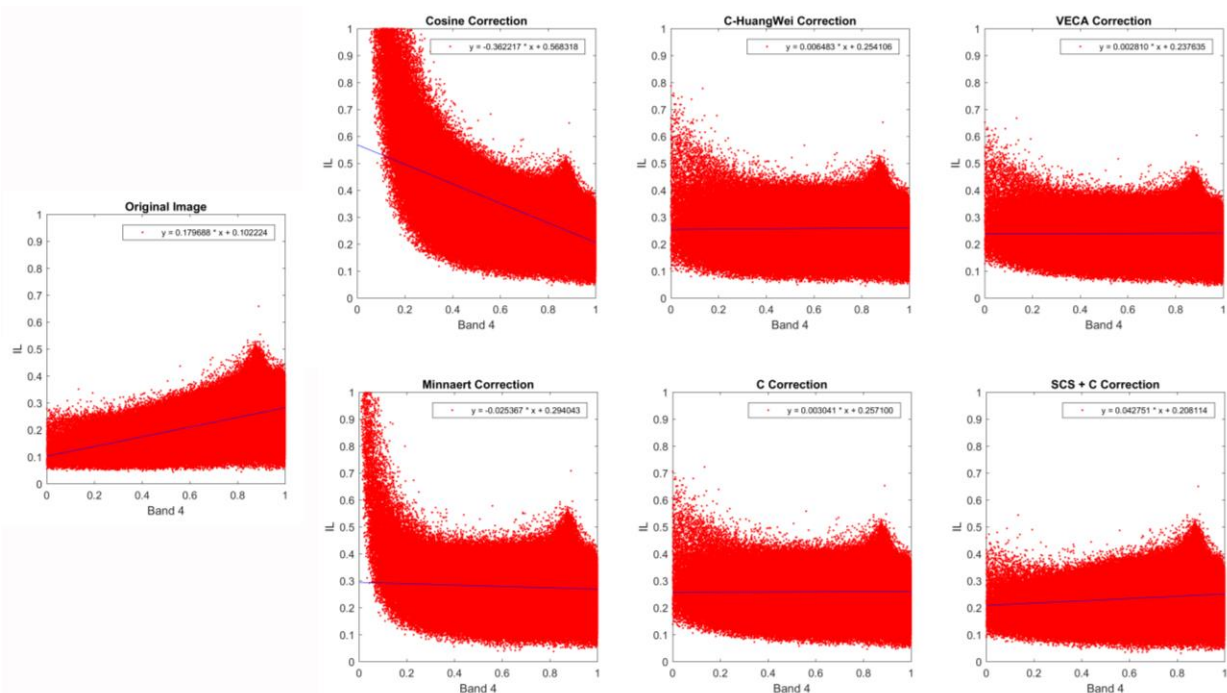


**Figure 5. Relation between IL & Reflectance for Near Infrared band of Sentinel-2**

The mean value of the image should not change much after topographic correction, inter-band variability should decrease after correction, and hence coefficient of variation should decrease. So, mean, standard deviation (SD) and coefficient of variation (CV) was calculated before and after the corrections as shown in table 4. The mean value of all the methods have not changed significantly as compared to the mean of original image. However the CV value of all bands after Cosine correction has changed significantly as given in Table 4, thus overcorrecting the topographic effects using Cosine method. This is also visible in Figure 6a where the overcorrection led to significant change in reflectance value. The Cosine correction method based on the Lambertian reflectance assumption, led to higher SD than some of the other methods. All the other 5 methods retained the similar mean value and SD as of original image for all bands. However out of these 5 methods, VECA has near similar mean and SD with respect to original image and it also has very less CV as was the case for C correction. Thus C-Huang Wei and Minnaert corrections have nearly similar statistics and could be considered as average models for topographic corrections in these conditions. While SCS + C has little better performance and could be considered as above average. Hence it can be ascertained that VECA and C are better performers than others. Therefore, from statistical analysis, it can be inferred that VECA and C method are best methods amongst all the discussed methods. Results of the correction along with original images are shown in Figure 6.

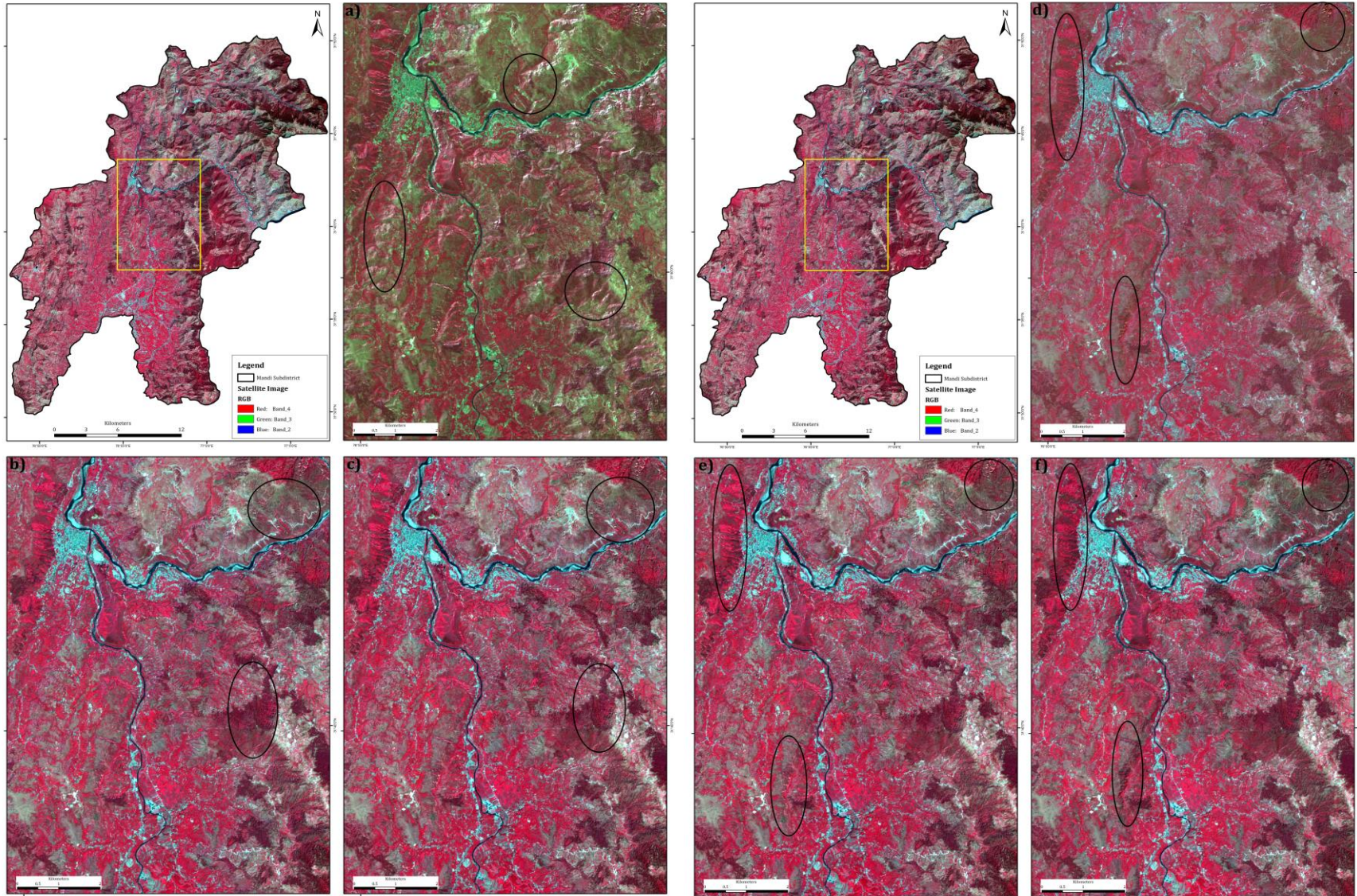


**Figure 6.** Results obtained after applying topographic correction original image. The significant changes for part of the image as shown by yellow box is given in different panes by using a) Cosine Correction; b) C-Huang Wei Correction, c) VECA Correction, d) Minnaert Correction; e) C Correction and f) SCS + C Correction

**Table 4. Image statistics showing mean, standard deviation (SD) and coefficient of variation (CV) calculated on all the bands of the original image and after all the corrections used in the study**

Bands / Methods	Original Image			"Cosine"			"C-Huang Wei"			"VECA"			"Minnaert"			"C"			"SCS + C"		
	Mean ( $\mu$ )	SD ( $\sigma$ )	CV	Mean ( $\mu$ )	SD ( $\sigma$ )	CV	Mean ( $\mu$ )	SD ( $\sigma$ )	CV	Mean ( $\mu$ )	SD ( $\sigma$ )	CV	Mean ( $\mu$ )	SD ( $\sigma$ )	CV	Mean ( $\mu$ )	SD ( $\sigma$ )	CV	Mean ( $\mu$ )	SD ( $\sigma$ )	CV
Band 1	0.097	0.015	15.408	0.120	3.398	2841.137	0.100	0.014	14.389	0.098	0.014	13.725	0.100	0.016	15.665	0.100	0.014	13.725	0.096	0.014	14.070
Band 2	0.095	0.019	19.882	0.115	3.007	2614.348	0.099	0.018	17.657	0.096	0.016	16.942	0.102	0.021	20.645	0.100	0.017	16.942	0.094	0.017	17.513
Band 3	0.082	0.028	34.293	0.099	2.721	2757.042	0.087	0.028	31.895	0.085	0.026	30.795	0.091	0.035	38.021	0.088	0.027	30.795	0.082	0.025	30.804
Band 4	0.240	0.050	20.737	0.286	5.084	1778.936	0.257	0.043	16.753	0.238	0.039	16.491	0.272	0.090	32.993	0.257	0.042	16.491	0.239	0.044	18.375

It is evident from Figure 6 that these methods did carry out topographic corrections. As indicated in the Figure 6, various locations in the original image has high topography which led to difference in spectral values irrespective of the similar land use class. Thus due to topography darker and brighter shades of similar vegetation is seen on either side of a mountains. These effects were reduced after topographic corrections. But as discussed earlier that Cosine correction is the worst performer, the output image is also very pale and the effect of topography is still present (Figure 6a). Similarly the effect of Minnaert correction (Figure 6d) shows reduction in brightness of the image and the contrast is reduced. Some locations where these changes are visible are marked in Figure 6. The other 4 methods gave similar results. But out of them VECA (Figure 6c) and C correction (Figure 6e) shows the best result visually. Both these methods did not develop much artifacts (visible when higher zoom is applied) as compared to other methods. Some of the locations where these subtle changes are prominent are marked on the image. Both of these methods outperform others by visual as well as statistical interpretation methods.

#### 4. CONCLUSIONS

Based on the comparative analysis, statistical and visual evaluation, we can draw the following conclusions on topographic correction methods performed on the Sentinel-2 image for Mandi sub-district region:

- i. The Cosine correction have the problem of overcorrection because it does not account for the non-Lambertian nature of the surface to the incident solar illumination and also for the contribution of indirect irradiance, so it is not suitable for correction of topographic effects in highly mountainous terrain as the Himalayas.
- ii. The remaining methods can be divided into two groups relative to their performance. VECA and C correction performed the best whereas C-Huang Wei, Minnaert, and SCS + C correction performed better than the Cosine methods.
- iii. Both statistically and visually, VECA and C correction have best results in highly rugged terrain. So it is advised that either of these methods could be applied for topographic corrections of satellite image of high mountain ranges such as Himalaya.

A wide variety of methods have been proposed in the literature, however, no methods are universally applicable. Also lack of standard and globally accepted models make it difficult to apply topographic corrections. As we see that the topographic effects in satellite images are influenced and determined by many other factors such as adjacent surface, atmospheric condition and land cover, so proper research should be carried out to check applicability of other methods with other images of the similar topography under different illumination conditions (very low sun elevation angle). A good correction method does not change reflectance value significantly but it cannot be applied universally.

#### 5. ACKNOWLEDGEMENT

The authors are greatly thankful to German Aerospace Center (DLR) for providing TanDEM-X digital elevation model of the study area through the project (Project No. DEM\_HYDR1925) sanctioned to Dr Dericks P. Shukla. We would like to thank European Space Agency for providing Sentinel-2 data free of cost.

## REFERENCES

- Balthazar, V., Vanacker, V., and Lambin, E. F., 2012. Evaluation and parameterization of ATCOR3 topographic correction method for forest cover mapping in mountain areas. *International Journal of Applied Earth Observation and Geoinformation*, 18:436-450.
- Colby, J. D., 1991. Topographic Normalization in Rugged Terrain. *Photogrammetric Engineering and Remote Sensing*, 57(5):531-537.
- Ekstrand, S., 1996. Landsat TM-Based Forest Damage Assessment: Correction for Topographic Effects. *Photogrammetric Engineering & Remote Sensing*, 62(2):151-161.
- Fan, Y., Koukal, T., and Weisberg, P. J., 2014. A sun-crown-sensor model and adapted C-correction logic for topographic correction of high resolution forest image. *ISPRS Journal of Photogrammetry and Remote Sensing*, 96:94-105.
- Gao, Y., and Zhang, W., 2007. Variable Empirical Coefficient Algorithm for removal of topographic effects on remotely sensed data from rugged terrain. *2007 IEEE International Geoscience and Remote Sensing Symposium*, Barcelona, 2007, pp. 4733-4736. doi: 10.1109/IGARSS.2007.4423917.
- Gao, Y., and Zhang, W., 2009a. LULC Classification and Topographic Correction of Landsat-7 ETM+ Image in the Yangjia River Watershed: the Influence of DEM Resolution. *Sensors*, 9(3):1980-1995.
- Gao, Y., and Zhang, W., 2009b. A simple empirical topographic correction method for ETM+ image. *International Journal of Remote Sensing*, 30(9):2259-2275.
- Gu, D., and Gillespie, A., 1998. Topographic normalization of Landsat TM images of forest based on subpixel Sun-canopy-sensor geometry. *Remote Sensing of Environment*, 64(2):166-175.
- Hantson, S., and Chuvieco, E., 2011. Evaluation of different topographic correction methods for Landsat image. *International Journal of Applied Earth Observation and Geoinformation*, 13:691-700.
- Jensen, J. R., 2005. *Introductory digital image processing: a remote sensing perspective*, Pearson Prentice Hall. Upper Saddle River, NJ. New Jersey, USA.
- Li, H., Xu, L., Shen, H., and Zhang, L., 2016. A general variational framework considering cast shadows for the topographic correction of remote sensing image. *ISPRS Journal of Photogrammetry and Remote Sensing*, 117:161-171.
- Meyer, P., Itten, K. I., Kellenberger, T., Sandmeier, S., and Sandmeier, R., 1993. Radiometric corrections of topographically induced effects on Landsat TM data in an alpine environment. *ISPRS Journal of Photogrammetry & Remote Sensing*, 48(4):17-28.
- Nichol, J., and Hang, L. K., 2008. The influence of DEM accuracy, on topographic correction of Ikonos satellite images. *Photogrammetric Engineering and Remote Sensing*, 74(1):47-53.
- Pimple, U., Sitthi, A., Simonetti, D., Pungkul, S., Leadprathom, K., and Chidthaisong, A., 2017. Topographic Correction of Landsat TM-5 and Landsat OLI-8 Image to Improve the Performance of Forest Classification in the Mountainous Terrain of Northeast Thailand. *Sustainability*, 9(2):258.
- Riaño, D., Chuvieco, E., Salas, J., and Aguado, I., 2003. Assessment of different topographic corrections in Landsat-TM data for mapping vegetation types. *IEEE Transactions on Geoscience and Remote Sensing*, 41(5):1056-1061.
- Richter, R., Kellenberger, T., and Kaufmann, H., 2009. Comparison of topographic correction methods. *Remote Sensing*, 1(3):184-196.
- Smith, J. A., Lin, T. L., and Ranson, K. J., 1980. The Lambertian Assumption and Landsat Data. *Photogrammetric Engineering & Remote Sensing*, 46(9):1183-1189.
- Soenen, S. A., Peddle, D. R., and Coburn, C. A., 2005. SCS+C: A Modified Sun-Canopy-Sensor Topographic Correction in Forested Terrain. *IEEE Transactions on Geoscience and Remote Sensing*, 43(9):2148-2159.
- Szantoi, Z., and Simonetti, D., 2013. Fast and Robust Topographic Correction Method for Medium Resolution Satellite Image Using a Stratified Approach. *IEEE Journal of Selected Topics in Applied Earth Observations and Remote Sensing*, 6(4):1921-1933.
- Teillet, P. M., Guindon, B., and Goodenough, D. G., 1982. On the slope-aspect correction of multispectral scanner data. *Canadian Journal of Remote Sensing*, 8:84-106.